Eur. Phys. J. D **28**, 259–266 (2004)
DOI: 10.1140/epjd/e2003-00297-y

**THE EUROPEAN PHYSICAL JOURNAL D**

# Prospect for BEC in a cesium gas: one-dimensional evaporative cooling in a hybrid magnetic and optical trap

S. Boussen, N. Hoang, S. Guibal[a], N. Zahzam, L. Pruvost, D. Marescaux, J. Pinard, and P. Pillet[b]

Laboratoire Aimé Cotton[c], CNRS II, Bâtiment 505, Campus d'Orsay, 91405 Orsay, France

Received 13 September 2002 / Received in final form 25 July 2003
Published online 2nd December 2003 – 

**Abstract.** Bose-Einstein condensation (BEC) in a atomic cesium gas prepared in a "low field seeker" Zeeman sublevel and confined in a magnetic trap has been thwarted by a high cross-section of inelastic spin-flip collisions. A recent experiment [1] succeeded in reaching BEC for cesium atoms using all optical methods and tuning the scattering length. We will discuss a hybrid magnetic and optical trap for cesium atoms in the true hyperfine ground state, the "high field seeker" Zeeman sublevel, $F = m_F = 3$. Although this trap allows only one-dimensional (1D) evaporative cooling, we show that a route towards BEC with such a trap should be possible. We present simulations of 1D evaporative cooling, which shows that a high phase space density (PSD) of 0.1 could be reached in less than 10 seconds.

**PACS.** 03.75.Hh Static properties of condensates; thermodynamical, statistical and structural properties – 05.30.Jp Boson systems – 32.80.Pj Optical cooling of atoms; trapping

## 1 Introduction

The usual route for Bose-Einstein condensation (BEC) in atomic vapours is to use non-dissipative magnetic traps coupled with the powerful technique of radio-frequency induced evaporative cooling, which increases the phase space density to beyond the BEC transition. Using this technique, BEC has been demonstrated for several alkali atoms [2–5]. With this approach in the case of the cesium atom, attempts to reach the BEC transition have failed. The reason for this is the large cross-section for inelastic collisions leading to the depolarization of the atoms in the trap. In order to cool, the forced evaporative method has to be coupled to a fast thermalization of the atomic sample through elastic collisions. Furthermore, the elastic collision cross-section must be significantly larger than the inelastic one. The elastic collisions guarantee cloud thermalization during the forced evaporation step, whereas the inelastic collisions lead to unnecessary trap losses, without decreasing the sample temperature. For both "low field seeker" Zeeman sublevels, $F = 4$, $m_F = 4$ and $F = 3$, $m_F = -3$, used in the previous experiments, the role of inelastic collisions to prevent realization of BEC has been clearly demonstrated [6–9]. Because of inelastic collisions, the cesium atom can be considered on one hand as a "bad" atom for cooling, but on the other hand as a very exciting system for several interesting reasons, such as the formation of cold molecules [10]. Understanding the cold collision processes is one of the motivations to push further the investigations for Cs BEC.

Despite these difficulties, a BEC of cesium atoms was recently achieved by the team of Grimm [1]. In this experiment, the way around the problem of inelastic collisions was to consider the lowest Zeeman sublevel $F = 3$, $m_F = 3$. For trapping such a "high magnetic field seeker" state the usual magnetic trapping schemes can not be applied since Maxwell's equations do not allow the existence of a magnetic field maximum in the vacuum (Wing's theorem). In this set-up, the cesium atoms are so confined by purely optical dipole forces provided by two crossed high power $CO_2$ laser beams. Furthermore a static homogeneous magnetic field is added for controlling the scattering length sign. More, this magnetic field allows to adjust the cross-section value during the BEC route. Note that the BEC approach in this experiment involves only optical methods: the evaporative cooling is performed by lowering the optical potential intensity.

A slightly different trap for cesium atoms in the same $F = 3$, $m_F = 3$ state is currently developed at laboratoire Aimé Cotton. The aim of this paper is to discuss the feasibility of BEC in such a set-up. The conservative trap we consider consists in a vertical Nd:YAG laser beam performing a 2D confinement combined to a magnetic field

[a] e-mail: samuel.guibal@lac.u-psud.fr
[b] e-mail: pierre.pillet@lac.u-psud.fr
[c] Laboratoire Aimé Cotton is associated with University of Paris-Sud.

gradient, provided by a pair of bars in which a large current is circulated, performing a vertical 1D confinement. The evaporative cooling can be obtained by a microwave frequency ramp to transfer the atoms from the trapped state, $F = 3$, $m_F = 3$, to a non trapped state $F = 4$, $m_F = 4$. Because the magnetic component of the trapping force is mainly along the vertical axis, contrary to BEC experiments on alkali atoms in magnetic traps, the evaporative cooling is neither a 3D nor 2D process but one-dimensional. This is expected to be less efficient, and it is unclear whether the run-away regime toward BEC can be achieved. The purpose of this article is to analyze the possibility to reach BEC with such a 1D evaporative cooling.

As demonstrated in the Grimm's experiment, an interesting feature provided by Cs atoms is the possibility of tuning the magnitude, and changing the sign of the scattering length associated with the Zeeman sublevel, $F = 3$, $m_F = 3$, by varying the magnetic field value. This possibility is due to the presence of a Feshbach resonance which allows one to change the positive scattering length in the range $0-1000a_0$ (where $a_0$ is the Bohr radius) by the addition of a magnetic field in the range of a few tens of gauss [11]. In the set-up described here, the magnetic configuration is designed in order to freely vary the field value at the position of the trapped cloud without modification of either the trap frequency or the position of the trap centre.

The paper is organized as follows. First, we describe the principle, geometry and characteristics of the trap for experimentally realistic parameters. Then, we numerically investigate the efficiency of 1D evaporative cooling in such a trap. The numerical model has been designed for simulating the collisional behaviour of cold trapped atoms including realistic values of the scattering length. In spite of the constraint of 1D evaporative cooling, the numerical data give a reasonable time for approaching the BEC transition, opening the possibility of achieving BEC in such a trap.

## 2 The trap

The design of the trap has mainly been imposed by experimental constraints. The non-dissipative trap shown in Figure 1 is created by two components: a magnetic apparatus which provides a vertical trapping force plus a tunable field, and one, far red detuned, laser beam which provides the horizontal trapping potential.

### 2.1 The magnetic field

In our set-up (Fig. 1), two different magnetic fields have to be considered, as they play a different role in the experiment. First, two horizontal parallel bars carrying opposite currents $I_t$ produce an inhomogeneous magnetic field $\overrightarrow{B_1}(x,z)$ (with $\overrightarrow{B_1}(x,z) = B_{1z}(x,z)\overrightarrow{e_z} + B_{1x}(x,z)\overrightarrow{e_x}$), the vertical gradient of which is equal to 30 G/cm at the trapping position $z = z_t$ in order to compensate for gravity. Second, a pair of Helmholtz coils (not represented in Fig. 1) with their axis along the vertical direction is used to realize a large homogeneous static magnetic field $\overrightarrow{B_0}$, which has two effects. First, as shown in Appendix A, it enables a trapping position at $z = z_t > 0$ (see Eqs. (A.6)). Second, as was mentioned in the introduction, it allows one to change the interactions between atoms by modifying the scattering length using Feshbach resonances. Recent measurements of the radiative collision loss rate carried out in the $F = 3$, $m_F = 3$ sublevel [11,12] have revealed the presence of a Feshbach resonance in the range 0–48 gauss and show that the scattering length $a$ is negative in the 0–18 G region with a large amplitude at zero field, and positive above 18 G, with a pole at 48 G. Therefore, the condition that $a > 0$, required to be able to observe a large stable condensate [4] leads us to choose the correct range of variation for $\overrightarrow{B_0}$ in order to produce a total magnetic field in the range of 18–100 G at the trapping position.

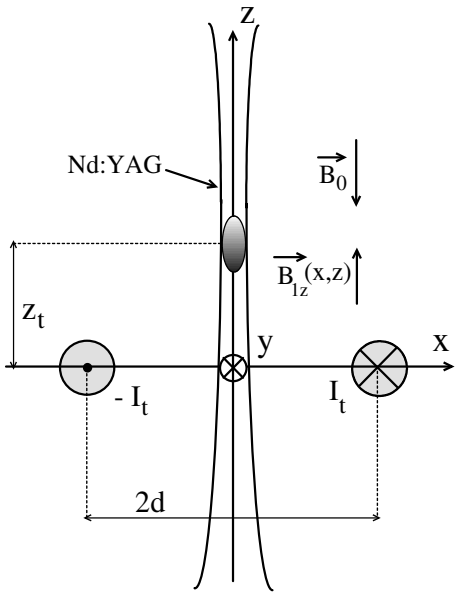


**Fig. 1.** The trap configuration in the $(xz)$ plane: $2d$ is the distance between the two bars, $z_t$ is the trap height. The circles represent a pair of conductors each of which carries a total current $I_t$. $\overrightarrow{B_{1z}}(x,z)$ is the $z$-component of the magnetic field $\overrightarrow{B_1}(x,z)$ created by the conductors, $\overrightarrow{B_0}$ is the homogeneous and constant magnetic field. In our experiment, $2d = 25$ mm, we have chosen $I_t \simeq 300$ A, in order to get $z_t \simeq 15$ mm. To get $z_t > 0$ we need to have $B_0 < -B_{1z}(0, z_t)$.

In view of the magnetic configuration, the total magnetic field is of the form (see Appendix A, and equations therein, for detail of the complete expression of $\overrightarrow{B}(x,z)$, Eq. (A.1)):

$$\overrightarrow{B}(x,z) = [B_0 + B_{1z}(x,z)]\overrightarrow{e_z} + B_{1x}(x,z)\overrightarrow{e_x} \qquad (1)$$

where $\overrightarrow{B_{1z}}(x,z)$ and $\overrightarrow{B_0}$ have an opposite direction (e.g. Eq. (A.2)).

Thus the magnetic potential experienced by an atom $V_B(x,z) = g_F \mu_B m_F |\overrightarrow{B}(x,z)|$, where $g_F$ is the Landé factor of the level ($g_{F=3} = -1/4$) and $\mu_B$ the Bohr magneton, can be expressed along the $z$-axis as:

$$V_B(0,z) = g_F \mu_B m_F |B_0 + B_{1z}(0,z)| = g_F \mu_B m_F \left| B_0 + B_w \frac{1}{1+z^2/d^2} \right| \quad (2)$$

where $B_w = \mu_0 I_t / \pi d$ represents $B_1(0,0)$ and $2d$ is the distance between the two bars.

This magnetic potential is superimposed on the gravitational potential, $V_g(z) = mgz$ with $m$ being the cesium atom mass, $g$ the local gravitational field. The tunable parameters of $V_B$ (i.e. $B_0$ and $B_w$) are chosen in order to get a minimum of the resulting potential $V_{\rm vert}(z) = V_B(0,z) + V_g(z)$ at $z = z_t > 0$ and a total magnetic field $B \equiv B(0,z_t)$ with an amplitude larger than 18 G at this value of $z_t$.

From expressions (Eqs. (A.10, A.4, A.5)) we can obtain $B_w(z_t)$, the trap oscillation frequency $\nu_t(z_t)$ and the range for $B_0$ in order to produce a total magnetic field larger than 18 G at $z_t$. One important feature of our magnetic set-up is that the trap position and the curvature depend only on the choice of $z_t$ and therefore on the value $B_w(z_t)$. They do not depend on the value of $B_0$ which only introduces a change of the total field and can modify the depth of the potential $\Delta V(z_t, B_0)$ (see Eqs. (A.7, A.9)). Consequently, by changing $B_0$, we should be able to tune the value of the scattering length without affecting either the trapping position or the trapping frequency.

Figures 2a–2c show the variations of these parameters for $2d = 25$ mm and are used to determine their value for the experiment. We have plotted Figure 2a $B_w$ and $\nu_t$ versus $z_t$, and in Figure 2b $B_0$ and $\Delta V$ versus $z_t$ and $B$. Figure 2c shows the variation of the potential $V_{\rm vert}(z)$ along the $z$-axis for $z_t = 15$ mm corresponding to $B_w = 97.2$ G, $\nu_t = 4.75$ Hz and for a set of $B_0$ values ($B_0 = -58, -78, -98$ gauss corresponding respectively to $B = -18, -38, -58$ gauss). In the following, we assume that the trapping position is located at $z_t = 15$ mm, with different values of $B$ in order to vary the scattering length.

## 2.2 The dipole trap

The optical part of the trap consists in one laser beam propagating along the $z$-axis (as shown in Fig. 1) which ensures a 2D horizontal confinement.

The dipole trap makes use of an intense far-off-resonance red detuned laser beam. The interaction of such a laser with the atoms consists mainly in a conservative attractive optical dipole force, scaling as the beam intensity and the inverse of the detuning between the laser frequency and the atomic transition frequency. The dissipative force, due to photon absorption, is negligible at a large value of the laser detuning, since it scales as the inverse of the square of the detuning. The resulting force is then assumed to be conservative.

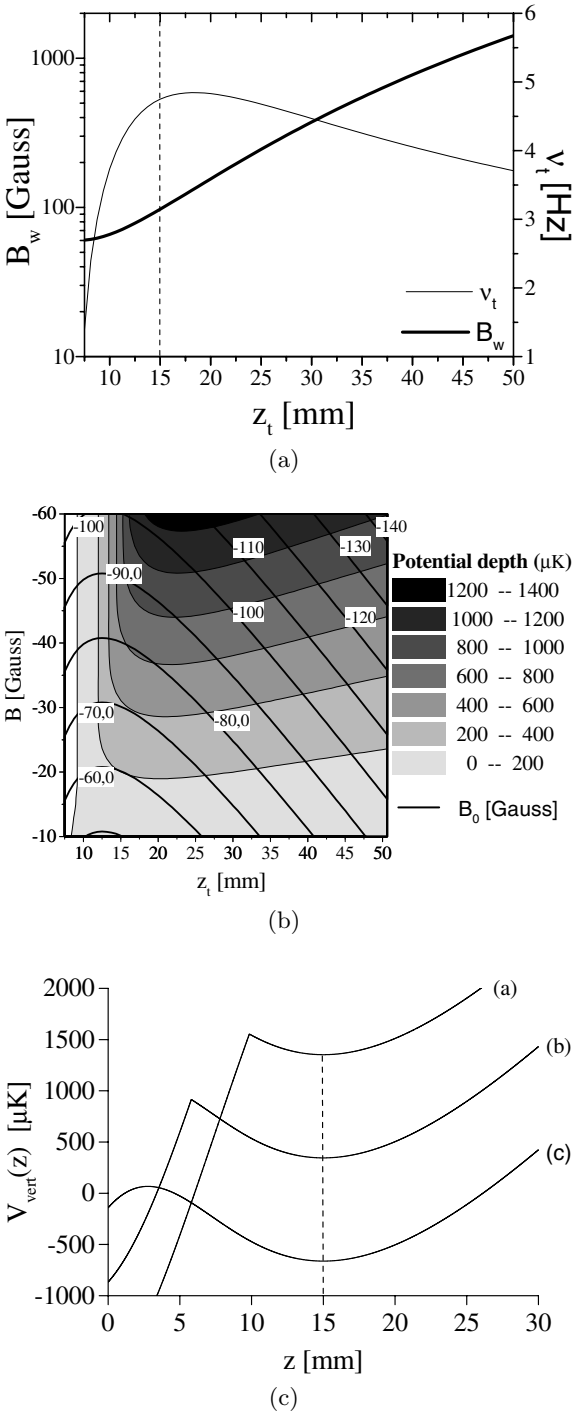


**Fig. 2.** (a) $B_w$ (bold line) and $\nu_t$ versus $z_t$ for $2d = 25$ mm where $B_w = \mu_0 I_t / \pi d = B_1(0,0)$ represents the maximum of the magnetic field (along the $z$-axis) created by the pair of bars and reached at $z = 0$. For $z_t \simeq 15$ mm (dashed line), we find $B_w = 97.2$ G and $\nu_t = 4.75$ Hz. (b) The total magnetic field $B \equiv B(0,z_t)$ at $z = z_t$ and the vertical potential $\Delta V$ (grey scale) versus $z_t$ and versus $B_0$ (bold line). For $z_t \simeq 15$ mm and $B_0 = -80$ G, we find $B = -40$ G, and $\Delta V = k_B 570$ $\mu$K. (c) The vertical potential $V_{\rm vert}(z) = V_B(0,z) + V_g(z)$ along the $z$-axis for $B = B(0,z_t) = -18$ G (a), $-38$ G (b), $-58$ G (c). The dashed line represents the trapping altitude $z_t \simeq 15$ mm.

The dipole trap can be achieved with a high power far detuned laser, for example a Nd:YAG or a $CO_2$ laser. We have chosen to perform the dipole trap by using a 15 W, 1064 nm Nd:YAG Gaussian laser beam. The frequency detuning from the closest cesium transition at 894.6 nm ($D_1$-Line) is $\delta = 1.2 \times 10^7 \Gamma$, where $\Gamma = 2\pi \times 4.56$ MHz is the full width at half maximum (FWHM) of the 894.6 nm. At this stage we neglect the spontaneous emission due to the excitation by the Nd:YAG laser. This effect will be discussed in the last part "Discussion and conclusion" of this paper.

The beam size is chosen in order to match the usual dimension of a MOT and to provide a sufficiently strong confinement. The laser beam whose size is chosen to be $w_{xy} = 220$ $\mu$m ($1/e^2$ beam radius) at the altitude $z = z_t$, creates a Gaussian potential with a depth $U_{xy} = k_B 52$ $\mu$K. By taking the zero energy at $(0, 0, z_t)$, the dipole potential can be expressed as[1]:

$$V_D(x, y) \simeq U_{xy} \left( 1 - e^{-2\left(\frac{x^2+y^2}{w_{xy}^2}\right)} \right). \quad (3)$$

The dipole trap radial frequency in the vicinity of (0, 0, $z_t$) is:

$$\frac{\omega_{xy}}{2\pi} = \frac{1}{\pi w_{xy}} \sqrt{\frac{U_{xy}}{m}}. \quad (4)$$

With the given experimental parameters the frequency value is $\omega_{xy}/2\pi = 82$ Hz.

The total potential $V_{\rm tot}(x, y, z) = V_B(x, z) + V_g(z) + V_D(x, y)$ has been plotted in Figure 3 in the vicinity of the trap centre $(0, 0, z_t)$. As shown, the vertical laser beam provides a tight horizontal confinement whereas the magnetic confinement along the vertical axis is weak.

### 2.3 Conditions of the evaporative cooling

The atomic sample is polarized and trapped in the $|F = 3, m_F = 3\rangle$ Zeeman sublevel, which allows the use of radio-frequency induced evaporation. As a consequence of the experimental configuration, such an evaporation can only be one-dimensional as it can be only performed along the $z$ direction. It is known to be less efficient [13,14]. Such a 1D process will be further studied in the next section. Because the design of the trap allows a total magnetic field larger than 18 G at the trapping position, the splitting between adjacent hyperfine Zeeman levels within $F = 3$ manifold is greater than $k_B 300$ $\mu$K. Therefore, the population of excited spin states via inelastic two-body spin-flip transition is strictly forbidden at typical temperature for atomic clouds loaded from a magneto-optical trap (MOT).

In our trap it is possible to use a microwave dipole transition between the $|F = 3, m_F = 3\rangle$ sublevel to the $|F = 4, m_F = 4\rangle$ sublevel. Indeed, on one hand the associated resonance transition is $z$ dependent due to the magnetic field gradient, and on the other hand, the $|F = 4, m_F = 4\rangle$ level is a "low field seeker" level and is not trapped in the magnetic device at $z = z_t$. Furthermore, atoms in this state are expelled from the $z = z_t$ region and leave this region mainly along the $z$-axis because the potential is still attractive along the $x$- and $y$-directions.

[1] The Rayleigh distance of the laser beams equal to 14 cm is large enough compared to the size of the atomic cloud, to assume that the beam is "parallel" in the trapping area.

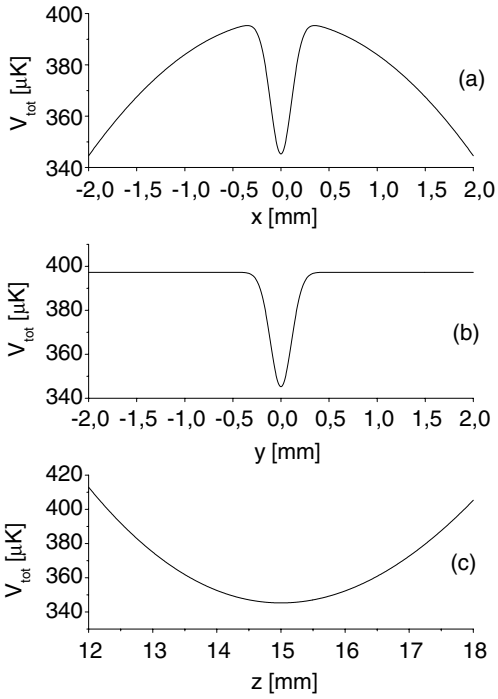


**Fig. 3.** The total potential $V_{\rm tot}(x, y, z) = V_B(x, z) + V_g(z) + V_D(x, y)$. (a) $V_{\rm tot}(x, 0, z_t)$ versus $x$ with $z_t = 15$ mm. There is a magnetic repulsion. The depth is around $k_B 50$ $\mu$K, $\omega_x/2\pi \simeq 80$ Hz. (b) $V_{\rm tot}(0, y, z_t)$ versus $y$. The depth is $k_B 50$ $\mu$K, $\omega_y/2\pi \simeq 80$ Hz. (c) $V_{\rm tot}(0, 0, z)$ versus $z$. The depth of the optical potential is $k_B 700$ $\mu$K, $\omega_z/2\pi \simeq 4.5$ Hz.

## 3 Quantitative analysis of 1D evaporative cooling

In order to quantitatively evaluate the 1D evaporation efficiency as a function of the scattering length, we have simulated the process using Bird's method [15]. This method, initially developed for molecular gas dynamics, has successfully been used to simulate evaporation processes [16,17] for BEC experiments.

In the dilute gas regime, particles move freely in the trapping potential and collide only occasionally. The collision duration is assumed to be very short in order to separate the particle motion from the collision. For that, we quantized the time into intervals $\Delta t$ (typically 100 $\mu$s) which is larger than the collision duration and smaller than the average time between two collisions. During $\Delta t$, the trajectory of each atom is determined by its motion in the harmonic potential. Indeed, for temperatures considered here (typically below 10 $\mu$K) Figure 3 shows that

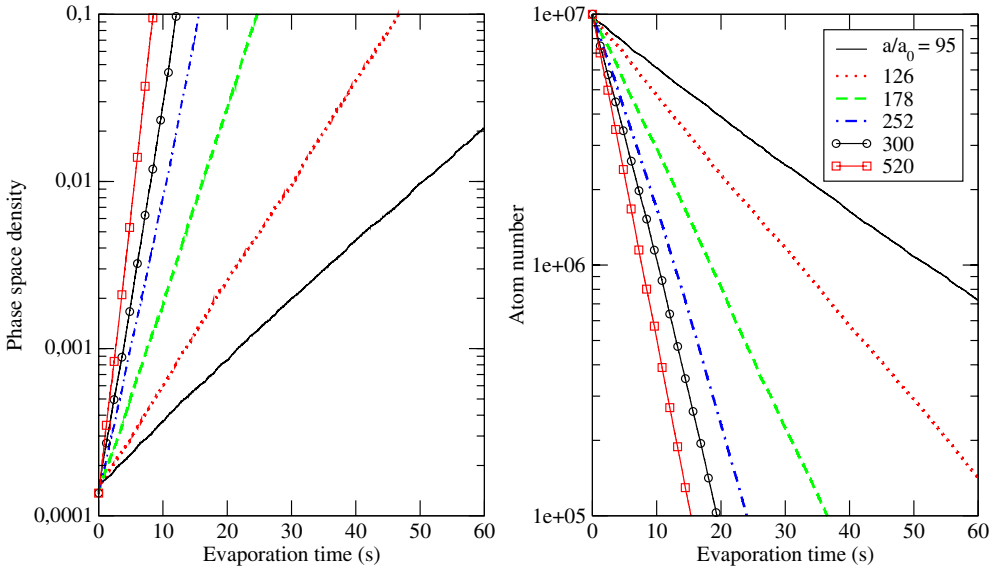


**Fig. 4.** Evolution of the phase space density (a) and the atom number (b) versus the evaporative time, for $\eta = 8$ and for a set of scattering length $a/a_0 = 95, 126, 178, 252, 300, 520$.

the harmonic approximation of the potential can be considered as correct. Therefore, we assume that the trap is characterized by two frequencies: $\omega_z/2\pi$ for the motion along the $z$-axis and $\omega_r/2\pi$ in the transverse plane (since $\omega_x$ and $\omega_y$ are very similar in our trap). Therefore, the atom indexed $i$ is exactly described by a set of amplitudes $a^i_{x,y,z}$ and a set of phases $\phi^i_{x,y,z}$ which give the atom position and velocity. The position is given by:

$$\begin{pmatrix} x^i(t) \\ y^i(t) \\ z^i(t) \end{pmatrix} = \begin{pmatrix} a^i_x \cos(\omega_r t + \phi^i_x) \\ a^i_y \cos(\omega_r t + \phi^i_y) \\ a^i_z \cos(\omega_z t + \phi^i_z) \end{pmatrix}. \quad (5)$$

Knowledge of the position and velocity avoids the need to solve the differential equations of the atom motion and leads to an enormous saving of calculation time. The collisions are assumed to be instantaneous. At every time step $\Delta t$ we check whether the atoms collided or not. We do not actually check the collision between all atoms because it is time consuming. The $N$ atoms are classified in an array of altitude and then we do the check process only between neighbours in this array (typically 100 neighbours). Thus the time of calculation scales as $N\ln(N)$ and not $N^2$. If a collision occurs, we consider the center of mass referenced with respect to the two particles. In this reference we randomly choose the angle between the final relative speed vector $\overrightarrow{v_r}^f$ and the initial relative speed vector $\overrightarrow{v_r}^i$. We also assume that atoms collide only in the $s$-wave regime so that the diffusion is isotropic. We also consider only elastic collisions so that the magnitude of the relative speed vector is preserved during the collision.

Using these features, we are able to simulate a few thousand atoms trapped in an anisotropic potential. However, for calculation time duration reasons it is impossible to simulate the dynamics of a few million atoms. Bird's method tackles this problem by considering "macro atoms". We simulate the dynamics of $N = N_{\rm real}/q$ atoms where $N_{\rm real}$ is the real trapped atoms number and $q$ a power of 2 factor (we choose $q = 1024$). In order to maintain the dynamics of the gas we consider the macro atom "$q$-time" bigger than the real one: the two body collisional cross-section between macro atoms $\sigma$ is taken to be $\sigma = q\sigma_{\rm real}$. Each macro atom has the same dynamic characteristics as $q$ real atoms. One difficulty of Bird's method appears in the case of evaporative cooling, which is that, during the evaporative process, the cloud looses atoms. We may assume that 10000 atoms are sufficient to represent our trapped gas but after losing 99% of them, it is less reasonable to build a statistical model on 100 atoms. In order to correct this problem, we use a trick from reference [8], which consists of refilling the trap after it has lost half of its trapped atoms. This can be done by duplicating the remaining atoms into clones having exactly the same characteristics but located symmetrically with respect of the centre of the trap (the speed is also taken symmetrical). The cross-section is then divided by a factor 2 in order to maintain the dynamics.

In usual evaporation models, the potential is truncated at an energy $E = \eta k_B T$ where $T$ is the temperature of the trapped sample. However, in the set-up described herein, the potential truncation is actually performed in one dimension along the $z$-axis at an altitude $z = \pm Z_{ev}$. Thus in our calculation we choose to define the evaporation surface $z = \pm Z_{ev}$ by the following relation: $m\omega_z^2 Z_{ev}^2 = \eta k_B T_z$, where $k_B T_z$ is the mean total energy for the atomic motion along the $z$-axis. With this choice, we take into account that the evaporation can be fast enough to prevent an isotropic thermal equilibrium of the sample. Of course if the thermalization rate is fast enough, one finds the usual definition with $T_z = T$. During the evaporation process, $\eta$ is kept constant. Although it may not be the optimized way, it gives a good indication of the cooling efficiency.

Figure 4 shows typical evaporation calculations, considering $10^7$ initial atoms at a temperature of 5 $\mu$K with $s$-wave scattering length $a/a_0$ ranging from 95 to 520 and $\eta = 8$. Each simulation was performed on a standard

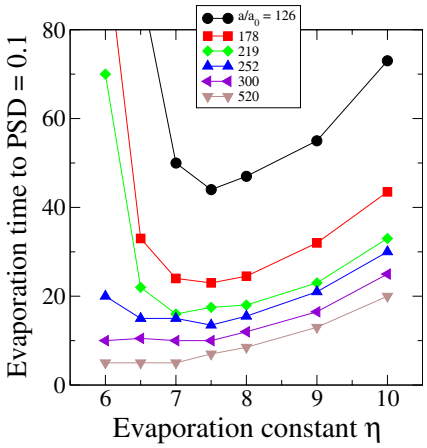


**Fig. 5.** Evaporation time to reach a phase-space density of 0.1 as a function of the evaporation constant $\eta$ for a set scattering length $a/a_0 = 126, 178, 219, 252, 300, 520$.

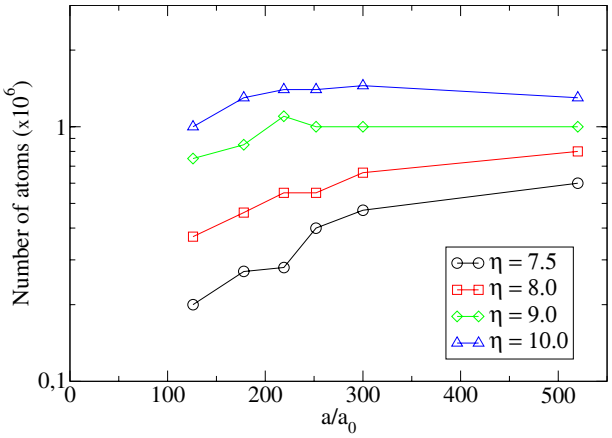


**Fig. 6.** Number of atoms remaining when a phase space density of 0.1 is reached as a function of the scattering length and for a set evaporation constant $\eta > 7$.

personal computer (P4 2.4 GHz CPU running linux) during typicaly 10 hours. Since our model is purely classical, the calculation is stopped when the phase-space density (PSD) reaches 0.1. Under these initial conditions, a PSD equal to 0.1 can be achieved in less than 10 s for $a/a_0 = 520$, showing that despite the 1D evaporation scheme, BEC could be reached within a reasonable evaporation time.

Since the experimental set-ups on Cs offers the possibility of varying the cross-section, we studied the evaporative cooling efficiency for several values of $a/a_0$. The second parameter of interest is the truncation constant $\eta$. The most relevant value derived from the numerical calculation is the time $t_{0.1}$ needed to reach a phase-space density of 0.1. Figure 5 shows the dependence of $t_{0.1}$ as a function of $\eta$ for various values of $a/a_0$ in the range 126–520. This range of cross-section is accessible for experimentally realistic magnetic field values (20–30 G). As expected, for a given value of $\eta$, the evaporative cooling efficiency is better for large cross-section[2]: the evaporative cooling process relies on the thermalization rate which itself depends on the value of the scattering length. The variation with the truncation constant $\eta$ can be described in terms of two regimes. First, for large values ($\eta > 8$ in the range of scattering length here-considered), the atom losses are sufficiently slow to allow the total energy to be uniformly distributed along the 3D. In that case, the cooling rate varies like the loss-rate. The loss-rate is decreasing as $\eta$ is increasing. On the other hand, one may be concerned by the number of atoms remaining at the end of the cooling sequence, then larger values of $\eta$ allows a selection of higher energy atoms to be evaporated from the trap. The cooling rate is decreased but the cooling efficiency per evaporated atom is better. This is illustrated by Figure 6 which shows the number of atoms remaining at each calculated point displayed in Figure 5. A different regime takes place for small values of $\eta$ ($\eta < 7$). In that situation, the evaporation rate is so high that the temperatures along the $z$-axis is much lower than along the transverse plane O$xy$. The evaporated atoms are lost without cooling down all the degrees of freedom which is strongly inefficient. Then not only the time for reaching $DEP = 0.1$ increases rapidly but also the number of remaining atoms decreases dramatically (for $\eta < 7$). Finally, it appears that the optimum value for $\eta$ (in terms of velocity) ranges between 7 and 8 and is slightly dependent on $a/a_0$. This result is close to the values usually used in experimental condition.

## 4 Discussion and conclusion

In this paper, we have proposed a hybrid magnetic and optical trap that confines high-field seeking states near a maximum of magnetic field, and analyzed the trap to assess its suitability to achieve BEC. The trap is not subject to Majorana spin flip and therefore turns off the two particle inelastic processes that have prevented previous attempts to reach Bose-Einstein condensation in cesium. A microwave frequency ramp may be implemented to force the evaporation cooling. Our simulation shows that although the evaporation is only one-dimensional, it is possible to reach a PSD of 0.1 within a time less than 10 s. We didn't push further the calculation because of the physical limitation of our model. This is made possible by the use of large cross-section. At this point it has been demonstrated both theoretically [18] and experimentally [1] that three-body collision could become important and prevent to reach the BEC transition. The way to overcome this problem is to lower the magnetic field to in order to reach lower values of the cross-section thus strongly reducing the three-body collision rate [1].

Using a classical collisional model, we have performed numerical simulations of 1D forced evaporative cooling induced by microwave transitions to an untrapped hyperfine

[2] However, if the cross-section becomes too large (typically $a/a_0 \gtrsim 1000$), a new regime appears known as hydrodynamic regime. In this regime, the evaporation efficiency decreases.

substate. We have shown numerically that the conditions for reaching a phase space density close to unity using the evaporative cooling procedure are experimentally realistic. Furthermore, the possibility of varying the Cs–Cs scattering length using a supplementary homogeneous magnetic field allows the experimental study of a BEC with tunable interactions. In our set-up, the existence of a magnetic gradient implies also a space dependence of the scattering length. However, this variation remains low at the cloud position since the magnetic gradient is only about 3 G/mm. Tunable interactions are of particular interest in the context of the formation of a molecular condensate since the use of a Feshbach resonance appears to be a promising way to transform efficiently a sample of cold atoms into a sample of cold diatomic molecules [19].

This work is supported by "Action Concertée Incitative Photonique" of the French research Ministry. The people involved in this work are members of the European Network "Cold Molecules" n° HPRN-CT-2002-00290. The authors thank Daniel Comparat for fruitful discussion and Duncan Tate for a critical reading of this manuscript.

## Appendix A: Calculation of the parameters of the potential $V_{vert}(z)$

The Biot-Savart formula in a static regime gives, for the magnetic field $\overrightarrow{B_1}$ created by two infinite wires along the $y$-direction carrying an opposite current $I_t$ and separated by a distance $2d$, the following expressions

$$B_{1z}(x,z) = \frac{\mu_0 I_t}{2\pi}\left(\frac{d-x}{(d-x)^2+z^2} + \frac{d+x}{(d+x)^2+z^2}\right)$$
$$B_{1x}(x,z) = \frac{\mu_0 I_t}{2\pi}\left(\frac{z}{(d-x)^2+z^2} - \frac{z}{(d+x)^2+z^2}\right). \quad \text{(A.1)}$$

To get a minimum for the potential $V_{\rm vert}(z)$ at $z = z_t > 0$ (a minimum at $z = 0$ is not desirable in an experiment because of laser beam shading by the wires), the two following conditions have to be satisfied:

$$B_0 < -B_{1z}(0,z_t) \quad \text{i.e.} \quad B_0 + B_w\frac{1}{1+z_t^2/d^2} < 0 \quad \text{(A.2)}$$
$$z_t > d/\sqrt{3}. \quad \text{(A.3)}$$

Under these conditions, and using equation (2), we can calculate the $z_t$ value where the potential $V_{\rm vert}(z) = V_B(0,z) + V_g(z)$ is minimal, and we obtain:

$$B_w = \frac{-mgd}{g_F\mu_B m_F}\frac{(1+z_t^2/d^2)^2}{2z_t/d}, \quad \text{(A.4)}$$

which defines $B_w(z_t)$.

To realize an adequate total field at $z_t$, $B = B(0,z_t) = B_{1z}(0,z_t) + B_0$ such as $|B| > 18$ G, $B_0$ has to be chosen so that:

$$B_0 < -18 - B_w\frac{1}{1+z_t^2/d^2} = -18 - \frac{-mgd}{g_F\mu_B m_F}\frac{1+z_t^2/d^2}{2z_t/d}, \quad \text{(A.5)}$$

which gives in the case of our experiment, for $z_t = 15$ mm ($B_w = 97.2$ G), $B_0 < -58$ G.

To find the expression for the depth of the potential $V_{\rm vert}(z)$, one has to determine the expression of its maximum $z_{\max}$. Indeed, in the range $0 - z_t$, $V_{\rm vert}(z)$ has a maximum for $z = z_{\max}$ as shown in Figure 2c. It is easy to show that, because $z_{\max}$ is close to zero, $z_{\max}$ is approximately found to be:

$$z_{\max} \sim \frac{d}{2}\left(\frac{-mgd}{g_F\mu_B m_F}\right)/B_w = d\frac{z_t/d}{(1+z_t^2/d^2)^2}. \quad \text{(A.6)}$$

This value is only obtained for high $|B_0|$ field, satisfying $B_0 \lesssim -B_w/(1+z_{\max}^2/d^2)$. In that case, the depth of the potential given by:

$$\Delta V(z_t) = -g_F\mu_B m_F B_w\left(\frac{1}{1+z_{\max}^2/d^2} - \frac{1}{1+z_t^2/d^2}\right) + mg(z_{\max} - z_t) \quad \text{(A.7)}$$

which does not depends on $B_0$.

For $B_0 \gtrsim -B_w/(1+z_{\max}^2/d^2)$, the potential has its maximum for the zero field value at:

$$z_{\rm zero} = d\sqrt{\frac{B_w}{-B_0} - 1} \quad \text{(A.8)}$$

and the depth of potential:

$$\Delta V(z_t, B_0) = g_F\mu_B m_F\left(B_0 + B_w\frac{1}{1+z_t^2/d^2}\right) + mg(z_{\rm zero} - z_t) \quad \text{(A.9)}$$

depends on $B_0$.

For $2d = 25$ mm, $z_t = 15$ mm, $z_{\max}$ is found to be $\sim 2.52$ mm, and for $B_0 < -93.4$ G, $\Delta V = k_B 729$ $\mu$K whereas for $B_0$ ranging from $-93.4$ to $-58$ G, $\Delta V$ varies from $k_B 729$ $\mu$K to $k_B 169$ $\mu$K.

In the vicinity of the minimum, the potential is well approximated by a harmonic potential $V_{\rm vert}(z) \approx V_{\rm vert}(z_t) + m\omega_t^2(z - z_t)^2/2$ and is characterized by the frequency $\nu_t = \omega_t/2\pi$:

$$\nu_t = \frac{1}{2\pi}\sqrt{\frac{g}{d}}\sqrt{\frac{3z_t^2/d^2 - 1}{(z_t/d)(z_t^2/d^2+1)}}. \quad \text{(A.10)}$$

## References

1. T. Weber, J. Herbig, M. Mark, H.-C. Nägerl, R. Grimm, Science **299**, 232 (2003)
2. M.H. Anderson, J.R. Ensher, M.R. Matthews, C.E. Wieman, E.A. Cornell, Science **269**, 198 (1995)

3. K.B. Davis, M.-O. Mewes, M.R. Andrews, N.J. van Druten, D.S. Durfee, D.M. Kurn, W. Ketterle, Phys. Rev. Lett. **75**, 3969 (1995)
4. C.C. Bradley, C.A. Sackett, J.J. Tollett, R.G. Hulet, Phys. Rev. Lett. **75**, 1687 (1995)
5. D.G. Fried, T.C. Killian, L. Willmann, D. Landhuis, S.C. Moss, D. Kleppner, T.J. Greytak, Phys. Rev. Lett. **81**, 3811 (1998)
6. J. Söding, D. Guéry-Odelin, P. Desbiolles, G. Ferrari, J. Dalibard, Phys. Rev. Lett. **80**, 1869 (1998)
7. D. Guéry-Odelin, J. Söding, P. Desbiolles, J. Dalibard, Europhys. Lett. **44**, 26 (1998)
8. D. Guéry-Odelin, J. Söding, P. Desbiolles, J. Dalibard, Opt. Expr. **2**, 323 (1998)
9. S.A. Hopkins, S. Webster, J. Arlt, P. Bance, S. Cornish, O. Marago, C.J. Foot, Phys. Rev. A **61**, 032707 (2000)
10. A. Fioretti, D. Comparat, A. Crubellier, O. Dulieu, F. Masnou-Seeuws, P. Pillet, Phys. Rev. Lett. **80**, 4402 (1998)
11. A.J. Kerman, C. Chin, V. Vuletić, S. Chu, P.J. Leo, C.J. Williams, P.S. Julienne, C.R. Acad. Sci Paris **2**, 633 (2001)
12. C. Chin, V. Vuletić, A.J. Kerman, S. Chu, Nucl. Phys. A **684**, 641c (2001)
13. P.W.H. Pinkse, A. Mosk, M. Weidemüller, M.W. Reynolds, T.W. Hijmans, J.T.M. Walraven, Phys. Rev. A **57**, 4747 (1998)
14. E.L. Surkov, J.T.M. Walraven, G.V. Shlyapnikov, Phys. Rev. A **53**, 3403 (1996)
15. G.A. Bird, *Molecular Gas Dynamics and the Direct Simulation of Gas Flow* (Clarendon, Oxford, 1994)
16. H. Wu, C.J. Foot, J. Phys. B **29**, L321 (1996)
17. H. Wu, E. Arimondo, C. Foot, Phys. Rev. A **56**, 560 (1997)
18. P.O. Fedichev, M.W. Reynolds, G.V. Shlyapnikov, Phys. Rev. Lett. **77**, 2921 (1996)
19. E.A. Donley, N.R. Claussen, S.T. Thompson, C.E. Wieman, Nature **417**, 529 (2002)